BCR-ABL alternative splicing as a common mechanism for imatinib resistance: evidence from molecular dynamics simulations

Tai-Sung Lee,[1] Wanlong Ma,[2] Xi Zhang,[2] Francis Giles,[3] Jorge Cortes,[4] Hagop Kantarjian,[4] and Maher Albitar[2]

[1]Consortium for Bioinformatics and Computational Biology, and Department of Chemistry, University of Minnesota, Minneapolis, Minnesota; [2]Department of Hematopathology, Quest Diagnostics Nichols Institute, San Juan Capistrano, California; [3]Division of Hematology, Cancer Therapy and Research Center, The University of Texas Health Science Center, San Antonio, Texas; and [4]Department of Leukemia, The University of Texas M. D. Anderson Cancer Center, Houston, Texas

Abstract

Rare cases of chronic myelogenous leukemia (CML) express high levels of alternatively spliced *BCR-ABL* mRNA with a 35-bp insertion (35INS) between *ABL* kinase domain exons 8 and 9. This insertion results in a frameshift leading to the addition of 10 residues and truncation of 653 residues due to early termination. Sensitive PCR-based testing showed that 32 of 52 (62%) imatinib-resistant CML patients in chronic phase and 8 of 38 (21%) in accelerated or blast crisis expressed varying levels of the alternatively spliced *BCR-ABL* mRNA. A three-dimensional structural model of the 35INS ABL kinase domain complexed with imatinib was built using homology modeling, followed by molecular dynamics simulations. Simulation results showed that the new residues cause a significant global conformational change, altering imatinib binding in a way similar to that of the T315I mutation and, therefore, providing resistance to imatinib that depends on the level of expression. [Mol Cancer Ther 2008;7(12):3834–41]

Received 5/20/08; revised 9/10/08; accepted 9/10/08.

Grant support: Partial support from the National Center for Supercomputing Applications (NCSA) under MCB050050N and MCB070003T grants. This work utilized the SGI Altix (Cobalt) system of NCSA and the Dell Linux Cluster (Longstar) of Texas Advanced Computing Center, The University of Texas at Austin, through the NCSA TeraGrid mechanism. T-S. Lee is a Consortium for Bioinformatics and Computational Biology fellow at the University of Minnesota. Computational resources at Minnesota Supercomputing Institute are utilized.

The costs of publication of this article were defrayed in part by the payment of page charges. This article must therefore be hereby marked *advertisement* in accordance with 18 U.S.C. Section 1734 solely to indicate this fact.

Requests for reprints: Tai-Sung Lee, Consortium for Bioinformatics and Computational Biology and Department of Chemistry, University of Minnesota, 207 Pleasant Street Southeast, Minneapolis, MN 55455. Phone: 612-625-6317; Fax: 612-625-6317. E-mail: leex2750@umn.edu

doi:10.1158/1535-7163.MCT-08-0482

Introduction

Chronic myelogenous leukemia (CML) is characterized by the t(9;22)(q34;q11) chromosomal translocation (1–5), which leads to production of the breakpoint cluster region-Abelson (BCR-ABL) fusion oncoprotein. BCR-ABL contains a constitutively activated tyrosine kinase domain that plays a role in malignant transformation and triggers CML (6, 7). Imatinib is the current first-line treatment for CML and acts by inhibiting the BCR-ABL tyrosine kinase (8–10). However, resistance to imatinib remains a major obstacle to the successful management of this disease. Primary and secondary resistance occur at varying rates, depending on the stage of diseases. Primary resistance has been reported in chronic, accelerated, or blastic phase at rates of 3%, 9%, and 51%, respectively (11, 12). Whereas approximately 35% to 45% of patients with imatinib resistance are found to have *ABL* mutations, significant numbers have no such mutations (13). Most of the reported mutations disrupt critical contact points between imatinib and the tyrosine kinase receptor domain (14–17). The T315I mutation (18, 19) and some mutations affecting the so-called P-loop of BCR-ABL confer a greater level of resistance to imatinib (16, 17, 20) and even the new tyrosine kinase inhibitors that are currently used and tested in these patients (12, 21). The role of Src family kinases has received particular interest as a possible mechanism for imatinib resistance (22), and overexpression and activation of the LYN kinase has also been implicated (23).

Here we report the expression of an alternatively spliced *BCR-ABL* mRNA found mainly in patients resistant to imatinib. Four similar cases have been reported (24, 25). The alternative splicing, resulting from an insertion of 35 nucleotides from intron 8 between exons 8 and 9, changes the reading frame and leads to expression of a truncated protein.

To understand the possible effects of the insertion, we used a homology modeling technique to model the three-dimensional structure of the resulting mutated ABL protein complexed with imatinib, followed by large-scale, long-time (30 ns) molecular dynamics simulations. A significant conformational change was observed in these simulations, and detailed analyses of imatinib binding were done. Here we present significant insights from these analyses that would not have been attainable with static models.

Materials and Methods

Patients and Samples

Peripheral blood samples from CML patients with and without imatinib resistance were tested for *ABL* kinase mutation. Some of the samples were from patients with resistance to dasatinib and nilotinib as well. Testing was

done with an Institutional Review Board–approved protocol. The majority of the tested samples were fresh, but a significant number were frozen cells in freezing mix stored at −70°C.

ABL Kinase Mutation Analysis by Direct Sequencing

Testing for *ABL* kinase mutations has been previously reported (26). Briefly, an 863-bp reverse transcription-PCR product encompassing the kinase domain of BCR-ABL was amplified using a forward primer that annealed in *BCR* exon b2 and a reverse primer that annealed at the junction of *ABL* exons 9 and 10. The products were sequenced in forward and reverse directions using dye terminator chemistry and an ABI sequencer (Applied Biosystems).

Sensitive Method for the Detection and Quantification of the Alternatively Spliced *BCR-ABL*

BCR-ABL fusion transcripts were amplified from CML patients' RNA by first-round reverse transcription-PCR using a forward primer that annealed in *BCR* exon b2 and a reverse primer that annealed at the junction of *ABL* exons 9 and 10. The first PCR is to ensure that transcripts of the normal *ABL* gene are not analyzed. We then performed a nested PCR targeting the *ABL* exon 8-9 splice junction where the 35INS was observed. The wild-type transcript yields a 218-bp amplicon, whereas the 35INS transcript yields a 253 (218+35)-bp amplicon. The amplification products were resolved on a 3100 ABI Genetic Analyzer (Applied Biosystems) by fragment analysis. The percent of 35INS product of the total (peak height) was assessed, and all samples with >20% alternatively spliced transcript were confirmed by sequencing. Only samples with >5% alternatively spliced transcript are considered positive.

Splice Variant Prediction

Two exon prediction programs, GrailExp[5] and FGENES[6] (27), were applied to the sequences of exon 8, intron 9, and exon 9 of the wild-type and 35INS transcripts.

Homology Modeling

The MODELLER (version 9v2; ref. 28) software package was used to build the homology model for the 35INS variant. The crystal structure of the complex of the kinase domain of BCR-ABL (inactive form) and imatinib was used as the MODELLER template structure (chain A, PDB code: 1IEP; ref. 15). The mutated protein sequence and the wild-type protein sequence were aligned using the ClusterW web server[7] (29), and the aligned sequences were used as the input alignment for MODELLER.

Molecular Dynamics Simulation

The MODELLER model of 35INS was then used as the initial structure for molecular dynamics simulation. The simulated system contains 28,597 atoms (ABL, 4,207; imatinib, 68; water, 24,291; sodium ion, 19; chloride ion, 12). All preparation steps were done using the VMD package[8] (version 1.8.6; ref. 30). All molecular dynamics simulations were done using the NAMD package (version 2.6; ref. 31) with the CHARMM27 force field (32, 33). Full periodic boundary conditions were used along with the smooth particle mesh Ewald method (34). In all, a 20-ns molecular dynamics production simulation was done after a 10-ns solvent/ion equilibration simulation. More detailed information on simulation setup can be found in our previous work (35).

Results

Detection of the Alternatively Spliced Transcript Using Direct Sequencing

Based on direct sequencing, which has limited sensitivity (20%), and after testing *BCR-ABL* transcripts from a large number of CML patients (~1,800) with resistance to imatinib, we detected a 35-bp insertion mutation in 27 patients (1.5%; Fig. 1A). Most of these samples showed a mixture of mutant and wild-type transcripts (mixed genotype), although 4 (15%) showed 100% alternatively spliced transcript without residual wild-type transcript (Fig. 1A). Patients were all diagnosed with CML and most were classified as resistant after treatment with imatinib. Newly diagnosed patients and patients treated with IFN-α only were also studied. Some of imatinib-resistant patients were also resistant to nilotinib and dasatinib. Resistance was confirmed by cytogenetic and molecular studies. Sequence analysis showed that the 35-bp insertion is a normal sequence in the *ABL* intron 8 that is inserted between exon 8 and exon 9 (Fig. 2). The splice variant prediction results were obtained from GrailExp and FGENES (Table 1), both of which predicted that the 35-bp insertion will likely cause a new exon to be formed between the wild-type exon 8 and exon 9. This newly inserted sequence results in a reading-frame shift and hence a new protein sequence with 10 new residues beginning at position 475 and a stop codon at position 485 (Fig. 2).

Sensitive Quantitative Analysis of the Alternatively Spliced *BCR-ABL* mRNA

Direct sequencing has an overall sensitivity of ~20% and therefore would not have detected low-level transcripts. To increase sensitivity for detecting the alternatively spliced mRNA, we designed a reverse transcription-PCR assay that first amplifies the fusion transcript, and then used nested PCR with fluorescently labeled primers to amplify the segment between exons 8 and 9 encompassing the alternatively spliced segment. The amplification products are resolved using GeneScan (Fig. 1B). Unfortunately, not all samples from the 1,800 patients were available and testing with this sensitive method was done on the most recent samples. These samples were consecutive without any selection and only few (three) of these samples were positive by sequencing. The percentage of the alternatively spliced (relative to total *BCR-ABL* transcript) is calculated (Table 2). Expression of the alternatively spliced *BCR-ABL* was most common in patients with imatinib-resistant, chronic-phase CML (62%) and this was significantly higher

[5] http://compbio.ornl.gov/grailexp/
[6] http://www.softberry.com/berry.phtml
[7] http://www.ebi.ac.uk/Tools/clustalw/index.html
[8] http://www.ks.uiuc.edu/Research/vmd/

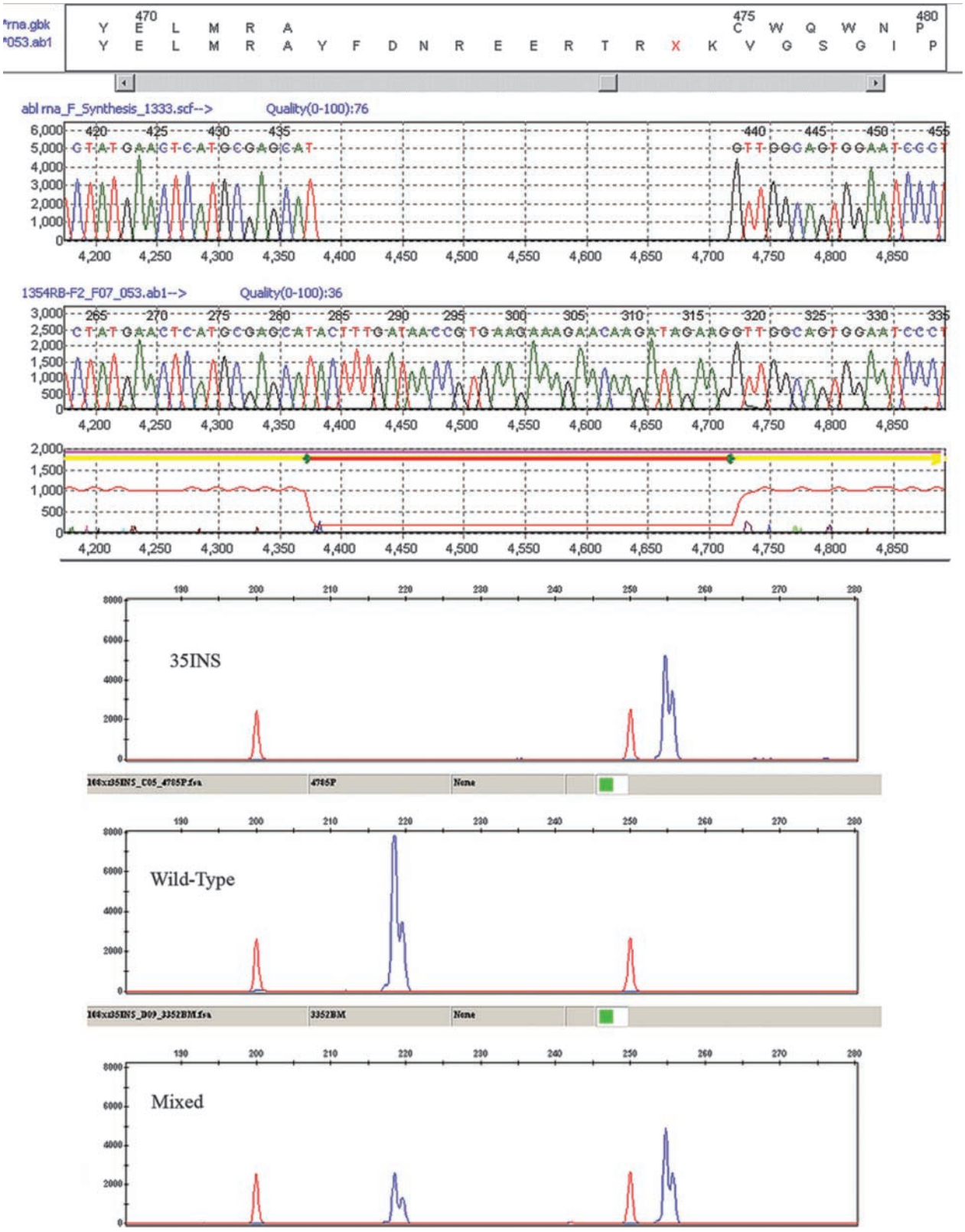

Figure 1. *Top,* example of sequencing results for *BCR-ABL* mRNA from peripheral blood cells showing the 35-bp insertion. *Bottom,* sensitive assay for detection of the 35-bp insertion using reverse transcription-PCR. The examples shown represent the expression of 100% alternatively spliced *BCR-ABL* (*top*), 100% wild-type *BCR-ABL* (*middle*), and a mixture of both (*bottom*).

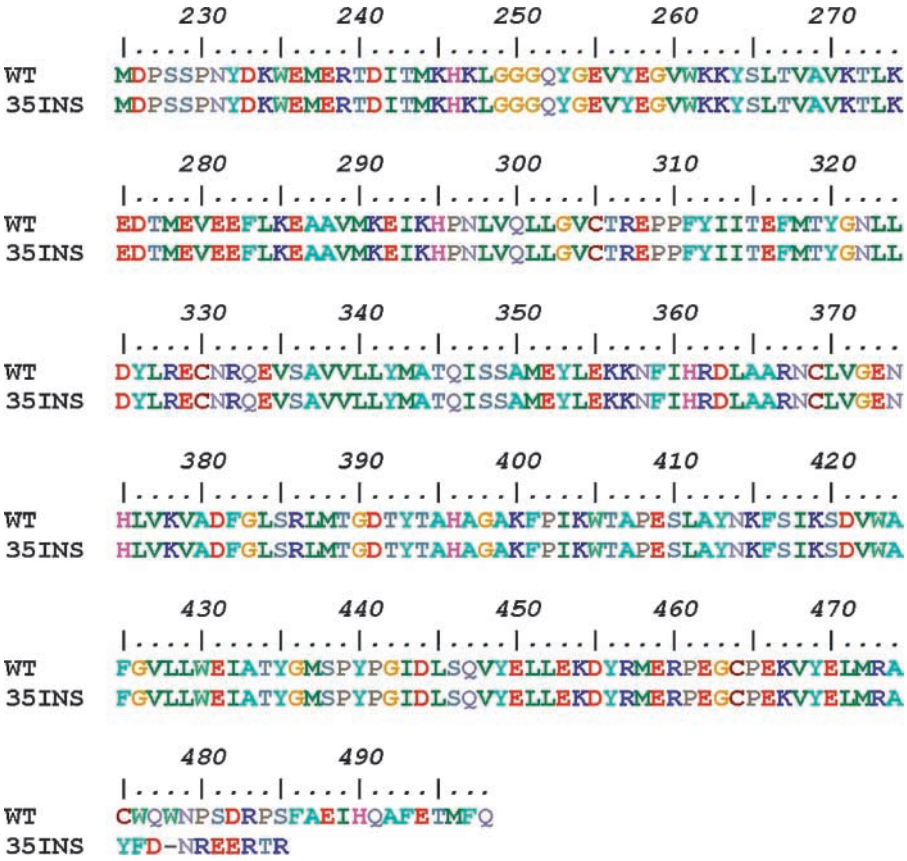

Figure 2. Protein sequence alignment for wild-type and 35INS ABL (obtained from ClustalW).

than in newly diagnosed patients ($P < 0.0001$, Fisher's exact test); only 21% of patients in the accelerated or blast phase expressed this variant (Table 2), which is also significantly higher than in newly diagnosed patients ($P = 0.04$). In contrast, most (28 of 29) newly diagnosed patients did not express the alternatively spliced *BCR-ABL* mRNA; the single untreated patient expressing the alternatively spliced transcript had primary resistance and died within 1 year of diagnosis. We also tested stored samples from patients who were treated with IFN-α but were resistant to therapy who had not been treated with imatinib; 20% of these patients expressed the alternatively spliced transcript, albeit at very low levels. The expression levels of the alternatively spliced *BCR-ABL* varied between patients (Table 2). The highest levels of expression were in patients with imatinib resistance in the chronic phase, followed by those in the accelerated or blast crisis. Among patients expressing the alternatively spliced transcript, 22% of those in the chronic phase and 63% of those in the accelerated or blast phase also carried a point mutation in the *ABL* gene.

Rare patients being treated with imatinib and considered responsive showed low-level expression of the alternatively spliced *BCR-ABL*. Considering only patients who remained molecularly positive for *BCR-ABL*, the alternatively spliced BCR-ABL was detected in 2 of 21 (10%) at 3 months, 1 of 20 (5%) at 6 months, 4 of 25 (16%) at 9 months, and 6 of 23 (26%) at 12 months of imatinib therapy. However, the levels of expression were low (<20%) in these patients. This trend suggests that patients who do not achieve molecular response are more likely to express the alternatively spliced *BCR-ABL*, and perhaps this explains their relative resistance to therapy. Our data indicate that approximately 50% to 60% of patients achieve molecular response by 6 months.

Based on longitudinal data, frequently the expression of the alternatively spliced *BCR-ABL* precedes the detection of

Table 1. Exon regions by two pattern-matching–based programs

35INS	GrailExp		FGENES		*ABL* exon 8		35INS	
Predicted exon region 1	73246	73413	73213	73305	73175	73327		
Predicted exon region 2	74478	74512	74478	74512			74478	74512

NOTE: The numbers denote the beginning and the end positions of the predicted exons (''GrailExp'' and ''FGENES''), and the observed exon positions [*ABL* exon 8 and 35-nucleotide insertion region (35INS)]. The numbering is based on the 35INS numbering scheme.

Table 2. Frequency of alternatively spliced *BCR-ABL* transcript (35INS) in various subgroups of CML patients

Patient subgroup	Patients tested	Positive (%)	% Expression, median (range)	Coexisting *ABL* point mutation (%)
Resistant, chronic phase	52	32 (62)	15 (5–100)	7 of 32 (22)
Resistant, accelerated/blast phase	38	8 (21)	17 (12–100)	5 of 8 (63)
Newly diagnosed	29	1 (3)	10	None
Previously treated with IFN-α (but not imatinib)	25	5 (20)	7 (5–20)	Not available

the ABL kinase mutation. Five patients with clinical resistance to imatinib, who developed ABL kinase mutation (L273M, G250E, T315I, F311L, and G250E), initially showed the expression of the alternatively spliced *BCR-ABL* 3 to 6 months before the detection of the mutation.

Taken together, these data indicate that expression levels and frequency of the alternatively spliced *BCR-ABL* are most strongly associated with imatinib resistance in the chronic phase of CML. Expression frequency and levels are less in patients with newly diagnosed CML and those treated with therapy other than imatinib (i.e., IFN-α), suggesting that imatinib selects for subclones that are capable of expressing the alternatively spliced *BCR-ABL*.

Homology Modeling and Molecular Dynamics Simulation

Conformational Changes. The modeled 35INS structure obtained from MODELLER package 9v2 is very similar to the template (i.e., wild-type) structure. The only major difference is a slight conformational change after residue 475 and truncation after residue 484. The homology modeling method used here predicted no global effect (Fig. 3, *left*) despite the global energy minimization done in the homology modeling process.

Molecular dynamics simulation showed very different results: After 20 ns, the 35INS protein exhibited major conformational changes in many regions of the *ABL* domain (Fig. 4, *right*). These changes were observed not only in the 35INS region (after residue 475) but also in almost every α-helix of the C-lobe. In the N-lobe, the C-helix moved into a different orientation with a position shift relative to imatinib. Our previous results suggested that long simulations are necessary for studying the effects of mutations in the BCR-ABL fusion protein (35). Simulation results for 35INS clearly show the need for long simulation times to detect these global conformational movements.

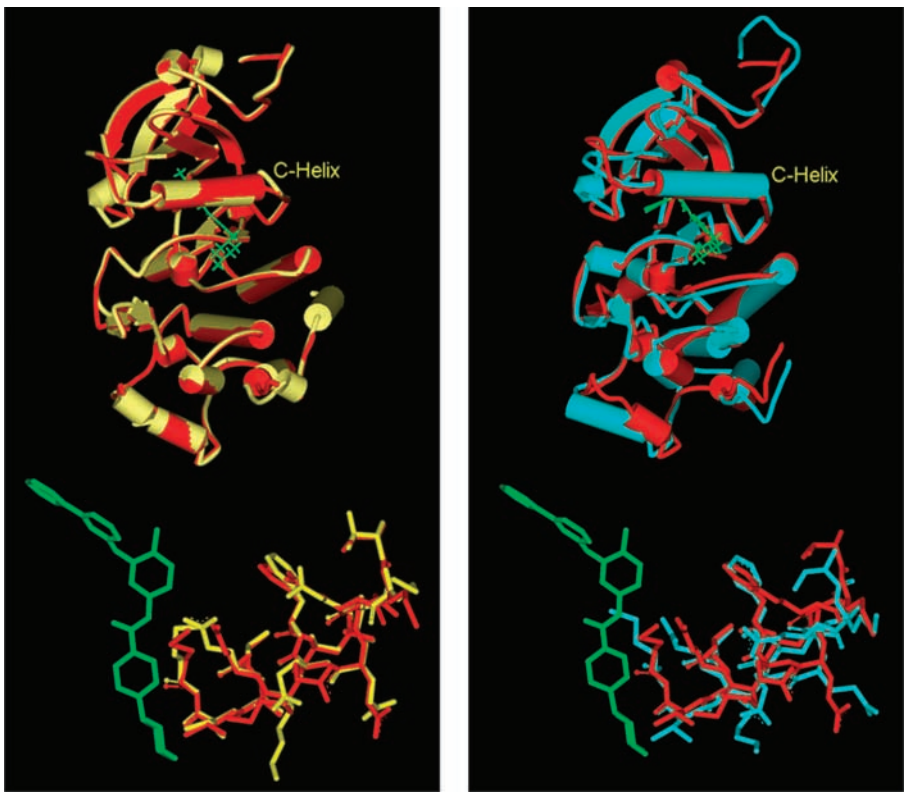

Figure 3. *Left,* the overlap schematic view (*top*) and heavy atoms of imatinib and C-helix (*bottom*) of wild-type ABL (*yellow*; PDB code: 1IEP) and the homology modeling structure (*red*). *Right,* the overlap schematic view (*top*) and heavy atoms of imatinib and C-helix (*bottom*) of the homology modeling structure (*red*) and the snapshot of molecular dynamics simulation at 20 ns (*light blue*). Imatinib is shown in green in both images. The backbone atoms of C-helix almost have the same positions in wild-type and homology modeling structures while their positions change significantly in the molecular dynamics structure.

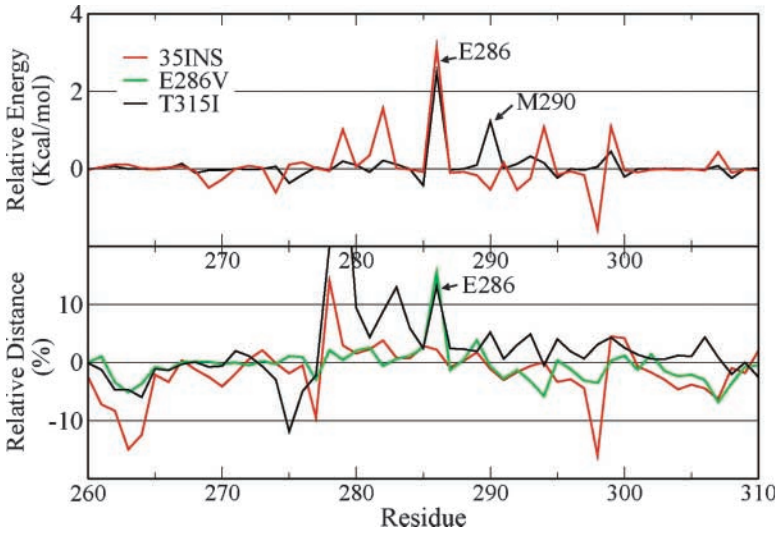

Figure 4. *Bottom,* the relative displacement percentage (compared with wild-type) for each residue from simulations of T315I and 35INS. The entries are calculated as follows: The average distance between the center of imatinib and the center of each residue is calculated first for each mutant. The relative distance change relative to the wild-type then is calculated for each residue in each mutant. For example, residue 280 of T315I shows ~40% increase in the plot, which means the distance between residue 280 and imatinib of T315I is higher than wild-type by ~40%. The same data for E286K, which only has local effect, are also shown for comparison. *Top,* relative nonbonding interaction energies (compared with wild-type, in kilocalories per mole) between each residue and imatinib from simulations of T315I and 35INS. The average is done over the last 15-ns simulations with a sampling frequency of 1 ps.

We have shown that reduction of the interaction between the C-helix and imatinib is the main cause of T315I-associated imatinib resistance (26). The relative movement patterns of the C-helix and nearby residues differ among the T315I, 35INS, and E286K (control comparison) mutants: T315I shows larger movement for the whole C-helix; 35INS shows large movements scattered in different regions; and E286K has larger movement only at E286. The different movement patterns of the C-helix suggest that the movement might be due to packing changes near T315 in the case of T315I, and to global conformational changes in many regions in the case of 35INS. The models shown in Fig. 4 (*bottom*), however, show only relative position changes between the centers of residues and the center of imatinib; they cannot be used to quantitatively describe the interaction changes. Small relative position changes, if only the centers are considered as in Fig. 4 (*bottom*), do not necessarily lead to small changes in interaction energies.

Interaction between the C-Helix and Imatinib. To further quantify the possible effect of the 35-bp insertion on imatinib resistance, we calculated the interaction energy between imatinib and each residue of the C-helix (Fig. 4, *top*). We previously showed that changes in interaction energy of E286 and M290 are the main contributors to T315I-associated drug resistance (26). Although the relative position changes of the C-helix for 35INS seem to be smaller than those of T315I, 35INS in fact exhibits larger interaction changes owing to the movement of the C-helix and weakened binding between imatinib and the C-helix. The calculated relative (to wide-type) interaction energy changes between C-helix (residues 278–290) and imatinib are 3.79 kcal/mol for T315I and 5.05 kcal/mol for 35INS; the total binding energies of imatinib are 6.84 kcal/mol higher than wild-type (35) for T315I and 7.65 kcal/mol higher than wild-type for 35INS.

Our previous binding energy analysis showed that the binding energy losses of T315I/imatinib are mainly due to the position changes of E286 and M290 relative to imatinib; T315I causes significant movement (>40% on residue 280) of the whole C-helix (278–290). Weisberg et al. (36) showed that, like imatinib, nilotinib has close contact with E286. As reported by von Bubnoff et al. (37), the position change of E286 due to T315I may be the reason for nilotinib resistance. Although dasatinib does not seem to interact directly with E286, T315I still causes dasatinib resistance (36). Our finding is also consistent with the suggestion of Levison et al. (22) that resistance to dasatinib is most likely due to the effects of T315I on the whole C-helix, which prevents formation of an active Src site.

All the statements above for T315I clearly also apply to 35INS, except that the interaction between M290 and imatinib is not reduced in the 35INS variant. Hence, based on our simulation results, we predict that 35INS will exhibit similar drug resistance. The shift of the whole C-helix may suggest that a new drug with a significantly different binding mode—probably one that has much less interaction with C-helix yet maintains the ability to block direct contact between the C-helix and the activation loop—is needed to overcome resistance due to T315I or 35INS.

Discussion

We report the finding that an alternatively spliced *BCR-ABL* transcript, resulting from the insertion of 35 bp between exons 8 and 9, is commonly expressed in patients with CML who develop resistance after exposure to imatinib. The alternative splicing leads to the insertion of 10 new residues at the C-terminus of the BCR-ABL protein; early translation termination due to a reading-frame shift causes deletion of the last 14 residues of the kinase domain (653 residues of the C-terminus).

The results of extensive molecular dynamics simulations indicate that these changes at the C-terminus cause major global conformational alterations in the protein. Although the C-helix does not seem to move in the same fashion seen with the T315I mutation, the substantial global movements

leading to changes in the imatinib-ABL interaction energy are similar. Thus, the resulting alternatively spliced protein should lead to imatinib resistance in a fashion similar to that seen in cells carrying the T315I mutation. However, in cells expressing the T315I mutant BCR-ABL, the cells expressing the T315I mutant protein is 100% of BCR-ABL protein and do not express wild-type BCR-ABL. In contrast, except in rare cases, the alternatively spliced *BCR-ABL* transcript generally accounts for a small proportion of total *BCR-ABL* expression. Therefore, we speculate that the expression of the alternatively spliced *BCR-ABL* confers a degree of resistance, rather than full resistance, and that the level of resistance may depend on the level of expression.

Cells with *ABL* mutation may evolve from a clone that expresses the alternatively spliced *BCR-ABL*. However, the concept of cells dependent on expressing the alternatively spliced *BCR-ABL* coexisting along with the cells carrying mutation may explain the frequent finding of missense mutant and wild-type cells in patients who are resistant to imatinib, particularly in the chronic phase. Among patients with the alternatively spliced variant, about one fifth of those in the chronic phase and more than half of those in the accelerated or blast phase had an additional *ABL* point mutation. It is possible that clones expressing the alternatively spliced *BCR-ABL* may give rise to clones that also carry an *ABL* mutation. It is also possible that cells dependent on expressing the alternatively spliced *BCR-ABL* coexist with cells carrying point mutations, particularly in the chronic phase.

These conclusions are supported by clinical data from patients with CML being treated with imatinib. We show that the proportion of patients resistant to imatinib who express the alternatively spliced *BCR-ABL* (62%) as compared with imatinib-negative patients (3%) is significantly high. We also show that patients who do not achieve molecular response show a clear trend toward increasing prevalence of expression of the alternatively spliced *BCR-ABL* (16% at 9 months and 26% at 12 months). Our findings also suggest that the same cells express both the alternatively spliced and the wild type, and it seems that the level of resistance depends on the level of expression. Low-level expression of the alternatively spliced transcript in each cell seems to confer a degree of resistance to imatinib. All these data along with the demonstration by molecular dynamics simulation that the new structure resulting from the 35INS renders the kinase domain resistant to imatinib lead to the conclusion that the 35INS is a major cause for resistance to imatinib.

The role of the alternatively spliced *BCR-ABL* in primary resistance to imatinib needs to be further explored with larger number of patents. Our data showed that one patient who expressed the alternatively spliced *BCR-ABL* showed primary resistance to imatinib, suggesting that this mechanism may play a role in primary resistance as well, but we need to study more patients.

The shown higher rate of concomitant mutation and the lower incidence of alternatively spliced *BCR-ABL* expression in the accelerated or blast phase (Table 2) suggest that additional molecular abnormalities are needed for the transformation to the accelerated or blast phase. Furthermore, premature translation termination of an mRNA is usually associated with poor mRNA stability (38, 39); this alternatively expressed *BCR-ABL* transcript is no exception. We observed a significant reduction in the relative ratio of alternatively spliced to wild-type *BCR-ABL* mRNA when samples were not processed promptly (data not shown). Additional studies are needed to explore the effect of the stability of this alternatively spliced *BCR-ABL* as well as the mechanisms that are responsible for its expression. Whether the expression levels or stability of this alternatively spliced *BCR-ABL* differ between stem cells and maturing cells and how these differences may influence minimal residual disease are important issues that require further investigation. Furthermore, *in vitro* models that express varying degrees of the mixture of wild-type and alternatively spliced fusion transcripts should be developed and studied for resistance to imatinib, as well as the new compounds being explored in treating patients with CML.

In summary, on the basis of our molecular dynamics simulations, the alternatively spliced *BCR-ABL* seems to confer resistance to imatinib. The alternatively spliced BCR-ABL protein may present alone or along with ABL mutations and may explain the coexistence of mutant and nonmutated leukemic cells in imatinib-resistant patients. We speculate that the relative levels of expression of the alternatively spliced *BCR-ABL* may be a factor in the degree of imatinib resistance sometimes seen in patients being treated with imatinib, but require longer time or higher dose to respond. Although the detection of 100% alternatively spliced mRNA in some patients indicates that the alternatively spliced RNA is translated adequately to maintain the leukemic cells and to provide resistance to imatinib, further studies are needed to specifically study this alternatively spliced and truncated BCR-ABL protein.

Disclosure of Potential Conflicts of Interest

No potential conflicts of interest were disclosed.

References

1. Kurzrock R, Gutterman J, Talpaz M. The molecular genetics of Philadelphia chromosome-positive leukemias. N Engl J Med 1988;319:990 – 8.

2. Faderl S. The biology of chronic myeloid leukemia. N Engl J Med 1999;341:164 – 72.

3. Deininger MW, Goldman JM, Melo JV. The molecular biology of chronic myeloid leukemia. Blood 2000;96:3343 – 56.

4. Goldman JM, Druker BJ. Chronic myeloid leukemia: current treatment options. Blood 2001;98:2039 – 42.

5. Druker BJ, O'Brien SG, Cortes J, Radich J. Chronic myelogenous leukemia. Hematology (Am Soc Hematol Educ Program) 2002;1:111 – 35.

6. Elefanty AG, Hariharan IK, Cory S. bcr-abl, the hallmark of chronic myeloid leukaemia in man, induces multiple haemopoietic neoplasms in mice. EMBO J 1990;9:1069 – 78.

7. Heisterkamp N. Acute leukemia in bcr/abl transgenic mice. Nature 1990;344:251 – 3.

8. Manley PW. Imatinib: a selective tyrosine kinase inhibitor. Eur J Cancer 2002;38:S19 – 27.

9. Deininger MW, Goldman JM, Lydon N, Melo JV. The tyrosine kinase inhibitor CGP57148B selectively inhibits the growth of BCR-ABL-positive cells. Blood 1997;90:3691 – 8.

10. Holtz MS. Imatinib mesylate (STI571) inhibits growth of primitive malignant progenitors in chronic myelogenous leukemia through reversal of abnormally increased proliferation. Blood 2002;99:3792 – 800.

11. Melo JV, Chuah C. Resistance to imatinib mesylate in chronic myeloid leukaemia. Cancer Lett 2007;249:121 – 32.

12. Hughes T. Monitoring CML patients responding to treatment with tyrosine kinase inhibitors—review and recommendations for harmonizing current methodology for detecting BCR-ABL transcripts and kinase domain mutations and for expressing results. Blood 2006;108:28 – 37.

13. Mahon FX. Selection and characterization of BCR-ABL positive cell lines with differential sensitivity to the tyrosine kinase inhibitor STI571: diverse mechanisms of resistance. Blood 2000;96:1070 – 9.

14. Nagar B. Structural basis for the autoinhibition of c-Abl tyrosine kinase. Cell 2003;112:859 – 71.

15. Nagar B, Bornmann WG, Pellicena P, et al. Crystal structures of the kinase domain of c-Abl in complex with the small molecule inhibitors PD173955 and imatinib (STI-571). Cancer Res 2002;62:4236 – 43.

16. Branford S. High frequency of point mutations clustered within the adenosine triphosphate-binding region of BCR/ABL in patients with chronic myeloid leukemia or Ph-positive acute lymphoblastic leukemia who develop imatinib (STI571) resistance. Blood 2002;99:3472 – 5.

17. Branford S, Rudzki Z, Walsh S, et al. Detection of BCR-ABL mutations in patients with CML treated with imatinib is virtually always accompanied by clinical resistance, and mutations in the ATP phosphate-binding loop (P-loop) are associated with a poor prognosis. Blood 2003; 102:276 – 83.

18. Gorre ME, Mohammed M, Ellwood K, Hsu N, Paquette R, Rao PN. Clinical resistance to STI-571 cancer therapy caused by BCR-ABL gene mutation or amplification. Science 2001;293:876 – 80.

19. Hochhaus A. Molecular and chromosomal mechanisms of resistance to imatinib (STI571) therapy. Leukemia 2002;16:2190 – 6.

20. Gorre ME, Ellwood-Yen K, Chiosis G, Rosen N, Sawyers CL. BCR-ABL point mutants isolated from patients with imatinib mesylate-resistant chronic myeloid leukemia remain sensitive to inhibitors of the BCR-ABL chaperone heat shock protein 90. Blood 2002;100:3041 – 4.

21. Mueller MC, Branford S, Radich J, et al. Response dynamics to nilotinib depend on the type of BCR-ABL mutations in patients with chronic myelogenous leukemia (CML) after imatinib failure. J Clin Oncol (Meeting Abstracts) 2007;25:7024.

22. Levinson NM, Kuchment O, Shen K, et al. A Src-like inactive conformation in the abl tyrosine kinase domain. PLoS Biol 2006;4:e144.

23. Donato NJ. BCR-ABL independence and LYN kinase overexpression in chronic myelogenous leukemia cells selected for resistance to STI571. Blood 2003;101:690 – 8.

24. Chu S-C, Tang J-L, Li C-C. Dasatinib in chronic myelogenous leukemia. N Engl J Med 2006;355:1062 – 3.

25. Laudadio J, Deininger MWN, Mauro MJ, Druker BJ, Press RD. An intron-derived insertion/truncation mutation in the BCR-ABL kinase domain in chronic myeloid leukemia patients undergoing kinase inhibitor therapy. J Mol Diagn 2008;10:177 – 80.

26. Ma W, Kantarjian H, Jilani I, et al. Heterogeneity in detecting Abl kinase mutations and better sensitivity using circulating plasma RNA. Leukemia 2006;20:1989 – 91.

27. Solovyev V, Salamov A. The Gene-Finder computer tools for analysis of human and model organisms genome sequences. Proc Int Conf Intell Syst Mol Biol 1997;5:294 – 302.

28. Fiser A, Sali A. Modeller: generation and refinement of homology-based protein structure models. Methods Enzymol 2003;374:461 – 91.

29. Larkin MA, Blackshields G, Brown NP, et al. Clustal W and Clustal X version 2.0. Bioinformatics 2007;23:2947 – 8.

30. Humphrey W, Dalke A, Schulten K. VMD: visual molecular dynamics. J Mol Graph 1996;14:33 – 8.

31. Phillips JC, Braun R, Wang W, et al. Scalable molecular dynamics with NAMD. J Comput Chem 2005;26:1781 – 802.

32. MacKerell AD, Jr., Brooks B, Brooks CL III, et al. CHARMM: the energy function and its parameterization with an overview of the program. In: Schleyer PvR, et al., editors. The encyclopedia of computational chemistry. Vol. 1. Chichester: John Wiley & Sons; 1998. p. 271 – 7.

33. Brooks BR, Bruccoleri RE, Olafson BD, States DJ, Swaminathan S, Karplus M. CHARMM: a program for macromolecular energy minimization and dynamics calculations. J Comput Chem 1983;4:187 – 217.

34. Essmann U, Perera L, Berkowitz ML, Darden T, Hsing L, Pedersen LG. A smooth particle mesh Ewald method. J Chem Phys 1995;103:8577 – 93.

35. Lee T-S, Potts SJ, Kantarjian H, Cortes J, Giles F, Albitar M. Molecular basis explanation of imatinib resistance of Bcr-Abl due to T315I and P-loop mutations from molecular dynamics simulations. Cancer 2008;112: 1744 – 53.

36. Weisberg E, Manley P, Mestan J, Cowan-Jacob S, Ray A, Griffin JD. AMN107 (nilotinib): a novel and selective inhibitor of BCR-ABL. Br J Cancer 2006;94:1765 – 9.

37. von Bubnoff N, Manley PW, Mestan J, Sanger J, Peschel C, Duyster J. Bcr-Abl resistance screening predicts a limited spectrum of point mutations to be associated with clinical resistance to the Abl kinase inhibitor nilotinib (AMN107). Blood 2006;108:1328 – 33.

38. Amrani N, Ganesan R, Kervestin S, Mangus DA, Ghosh S, Jacobson A. A faux 3′-UTR promotes aberrant termination and triggers nonsense-mediated mRNA decay. Nature 2004;432:112 – 8.

39. Behm-Ansmant I, Gatfield D, Rehwinkel J, Hilgers V, Izaurralde E. A conserved role for cytoplasmic poly(A)-binding protein 1 (PABPC1) in nonsense-mediated mRNA decay. EMBO J 2007;26:1591 – 601.